Magnetic order and electrical conductivity scaling of the spinel oxide $Mn_{0.5}Ru_{0.5}Co_2O_4$

R. N. Bhowmik* and R. Ranganathan†

Experimental Condensed Matter Physics Division, Saha Institute of Nuclear Physics, 1/AF, Bidhannagar, Calcutta 700064, India

(Received 30 July 2006; revised manuscript received 25 September 2006; published 18 December 2006)

We report the magnetic order and electrical (ac and dc) conductivity of bulk $Mn_{0.5}Ru_{0.5}Co_2O_4$ spinel oxide. The system is a ferrimagnet, which undergoes from ferrimagnetic to paramagnetic state above the Curie temperature (T_C) ~ 100 K. Low field ($\leqslant$100 Oe) measurement shows a peak at $T_p \approx 100$ K in zero field cooled (ZFC) magnetization, whereas field cooled magnetization continuously increases down to 2 K. As long as the applied magnetic field is not large enough in comparison with the coercive field, a sharp decrease in ZFC magnetization is always observed below T_p. The peak temperature at $T_p \approx 100$ K is shifted to lower temperatures by applying sufficiently large magnetic field. ac susceptibility (χ' and χ'') also shows a sharp peak at 100 K, which is independent of frequencies (0.5 Hz–1 kHz) of ac magnetic field (amplitude ~1 Oe). These observations, including other measurements, suggest strong pinning effects in domain wall dynamics. We have noted that electrical behavior of the system is significantly affected by the magnetic ordering of the spins. Our results have shown the contribution of short range interactions above T_C to the formation of small polarons. The system shows colossal magnetoresistance properties with a semiconductor to metallic transition below 80 K. A simple scaling law is used as a tool for the identification of short range magnetic interactions that may be difficult to determine using conventional magnetization experiments.

DOI: 10.1103/PhysRevB.74.214417 PACS number(s): 72.20.−i, 75.50.Pp, 75.10.−b

I. INTRODUCTION

Recently, many unconventional spinel oxides,[1–3] in addition to conventional ferrites, have generated renewed interest due to their potential applications in technology, as well as the observation of properties like ferrimagnetism, spin glass, superparamagnetism, metal-insulator transition and large magnetoresistance (CMR).[4–6] Spinel oxides, represented by formula unit AB_2O_4, are characterized by indirect (superexchange) interactions between cations among A (tetrahedral) and B (octahedral) sublattices. Magnetic moments in each of A and B sublattices are ferromagnetically aligned, whereas ferrimagnetic coupling between two sublattices is favorable for the exhibition of CMR effect in spinels. The discovery of colossal magnetoresistance (CMR) in many spinel compounds[6–9] has opened up a new field of research to understand the origin of large magnetoresistance (CMR) in oxide materials. $Mn_xCo_{3-x}O_4$ (Ref. 10) is one such spinel compound, which has shown CMR below their ferrimagnetic ordering temperature. Although most of the spinels are free from double exchange interactions between Mn^{3+} and Mn^{4+} ions, which plays an important role for the exhibition of CMR in perovskites[11] and pyrochlores,[12] the system $Mn_xCo_{3-x}O_4$ can be taken for the case study of a spinel containing Mn^{3+} and Mn^{4+} moments.[10,13–15] Earlier reports[16,17] suggested that bulk $MnCo_2O_4$ is a long range ferrimagnet with $T_C \sim 180$ K and its features are comparable in many ways to the ferromagnetic oxide $SrRuO_3$. For example, both compounds have shown CMR, both are anisotropic magnet, where magnetic behavior below T_C is controlled by domain wall movement. Small substitution of Ru by Mn in $SrRuO_3$ showed the appearance of short range magnetic order coexisting with long range ferromagnetic order.[18] Finally, antiferromagnetic order is observed in $SrMnO_3$. On the other hand, replacement of Mn by Ru in $MnCo_2O_4$ has shown antiferromagnetic spin-glass behavior in $RuCo_2O_4$.[19] These investigations suggest that substitution of Mn by Ru in $SrMnO_3$ and $MnCo_2O_4$ can exhibit a different kind of effect. As long as the spinel compound is concerned, $Mn_{1-x}Ru_xCo_2O_4$ could be an interesting system: (i) for understanding the role of Ru in $MnCo_2O_4$, (ii) for understanding the correlation between magnetic order and electrical conductivity, (iii) for considering a case study of short range interactions above T_C.[20]

We have selected 50% Ru substituted compound $Mn_{0.5}Ru_{0.5}Co_2O_4$, which is in between $MnCo_2O_4$ (ferrimagnet with metal-semiconductor behavior) and $RuCo_2O_4$ (insulating spin-glass). The neutron diffraction experiment[21] shows that cations in this compound are distributed as $(Co^{2+})_A[Co^{3+}(Mn^{3+})_{0.5}(Ru^{3+})_{0.5}]_BO_4$, where A and B represents tetrahedral and octahedral sublattices, respectively. First, we identify proper magnetic order of the system, and then establish a correlation between magnetic order and electrical conductivity. Such correlation has often been found in many CMR compounds employing dc magnetization, ac susceptibility and dc conductivity measurements. We believe that ac conductivity measurement can also be probed successfully for the proper understanding of magnetic order and the present work explores that possibility by a scaling analysis of ac conductivity data.

II. EXPERIMENT

Bulk $Mn_{0.5}Ru_{0.5}Co_2O_4$ (polycrystalline) sample was prepared by mixing the stoichiometric amounts of Co_3O_4 (99.5% from Fluka), MnO_2 (99.999% from Johnson Matthey), and RuO_2 (99.95% from Johnson Matthey) powders. The pellet form of the mixture was sintered at 950 °C for 24 hours and at 1400 °C for 18 hours with intermediate grinding and pelletizing. The heating and cooling rate was maintained at 2 °C per minute. The sample was characterized by x-ray diffraction using Cu $K\alpha$ radiation using Philips PW1710 diffractometer. The XRD data suggested cubic spi-

nel structure for the sample with lattice parameter ≈8.270 Å.

dc magnetization was measured, using SQUID magnetometer (Quantum Design), under the zero field cooled (ZFC) and field cooled (FC) conditions. ac susceptibility of the sample was measured in the frequency range 0.5 Hz–1.5 kHz at ac field amplitude $h_{rms} \approx 1$ Oe. The dc conductivity of the sample was measured using Keithley 2001 multimeter in the absence and presence of 8 kOe magnetic field. The real component of ac conductivity (σ_p) was measured in the frequency range $f=17$ Hz to 1 MHz at an ac electric field amplitude $\epsilon_0=1$ V using Quad Tech 7600 precision LCR meter. All the electrical measurements were carried out by a two-probe pressure contact technique using two sharp pointed end copper rods. The sample of dimension ~10 mm × 5 mm × 1.75 mm was placed tightly in between the rods so that separation between the pointed ends of the rods are 1.75 mm. Hence, the unwanted contact problem that has been encountered during ac conductivity measurement[22] can be avoided. The temperature was well controlled within ±0.1 K accuracy using Lakeshore temperature controller (model 330).

III. RESULTS

A. Magnetization

Temperature dependence of zero field cooled and field cooled magnetization are shown in Fig. 1. Figure 1(a) shows that zero field cooled magnetization (MZFC) and field cooled magnetization (MFC) for 10 Oe are merged above 150 K, whereas magnetic irreversibility between MZFC and MFC starts below 150 K, the temperature is denoted as magnetic irreversibility temperature T_{irr}. On further lowering the temperature, MZFC increases up to a peak at $T_p \approx 100$ K. Below 100 K MZFC shows a sharp decrease, whereas MFC continues to increase down to 2 K. To understand the nature of magnetic order at about T_p, we have measured magnetization at different fields of higher magnitude. We have noted that T_{irr} shifts to lower temperatures with the increase of measurement field. The observation of magnetic irreversibility below 45 K for 50 kOe field suggests that the system is not magnetically saturated even at 50 kOe. The MZFC vs temperature plot at selected fields [Fig. 1(b) (semilog scale)] shows that the peak position at $T_p \approx 100$ K is not significantly affected in the lower field range up to ~100 Oe. But, the peak position shifts to lower temperatures on further increasing the magnetic field (e.g., 200 Oe and more). The sharp decrease of MZFC is seen even for the measurement field 20 kOe below $T_p \sim 9$ K, whereas MZFC at 50 kOe does not show any decrease down to 2 K. Such a strong magnetic field dependence of T_p may indicate either a frustrated magnetic state (like spin glass/cluster spin glass) or an anisotropy ferrimagnet, the signature is already found in the appearance of a large magnetic irreversibility between MFC and MZFC below T_p.

The inverse of dc susceptibility ($1/\chi = H/M$) vs temperature plot [inset of Fig. 1(a)] above 100 K seems to be a hyperbola instead of a straight line. According to Néel's theory of ferrimagnetism[23] such curve above T_C follows the equation $1/\chi = (T-\theta_w)/C - \xi/(T-\theta)$, C is the Curie constant,

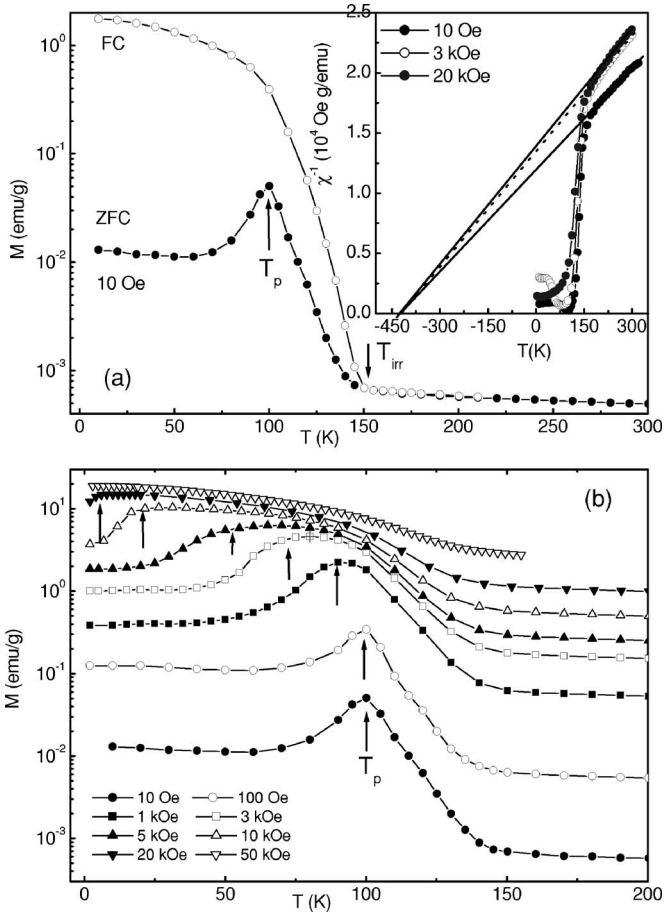

FIG. 1. (a) ZFC magnetization (MZFC) and FC magnetization (MFC) vs temperature (T) at 10 Oe. T_p and T_{irr} represents the peak temperature and irreversibility temperatures, respectively. Inset shows the inverse of dc susceptibility vs T for 10 Oe, 3 kOe, and 20 kOe data. Lines are a guide to the Curie-Weiss behavior above 150 K. (b) MZFC vs T for selected fields.

θ_w and θ are also constants. We find that $M(T)$ data above 150 K can be approximated to a Curie-Weiss law, $1/\chi = C/(T-\theta_w)$. The value of θ_w is nearly the same ~−420 K for $H=10$ Oe, 3 kOe, and 20 kOe. The negative value of the Curie-Weiss temperature (θ_w) indicates the dominance of antiferromagnetic exchange in the balance of the exchange interactions. However, the estimated values of Curie constant C are slightly field dependent, which is related to the field induced magnetic order at lower temperatures. On the other hand, the data below 150 K (below T_{irr}) deviate from the Curie-Weiss law with above parameters, and another slope intersects the temperature axis (where $1/\chi=0$) at a temperature close to 100 K. Such typical $\chi(T)$ behavior suggests that (ferri)magnetic ordering of the two (A and B) sublattices effectively gives rise to a ferromagnetic ordering below 100 K.[23]

To examine the spin-glass-like feature, we have measured ac susceptibility with close temperature interval in the range 80 K to 120 K ($T_p \pm 20$ K). The ac susceptibility [χ' in Fig. 2(a) and χ'' in Fig. 2(b)] shows a peak at about 100 K. The peak position does not show any noticeable shift in the frequency range 0.5 Hz to 1 kHz. The application of 1 kOe dc

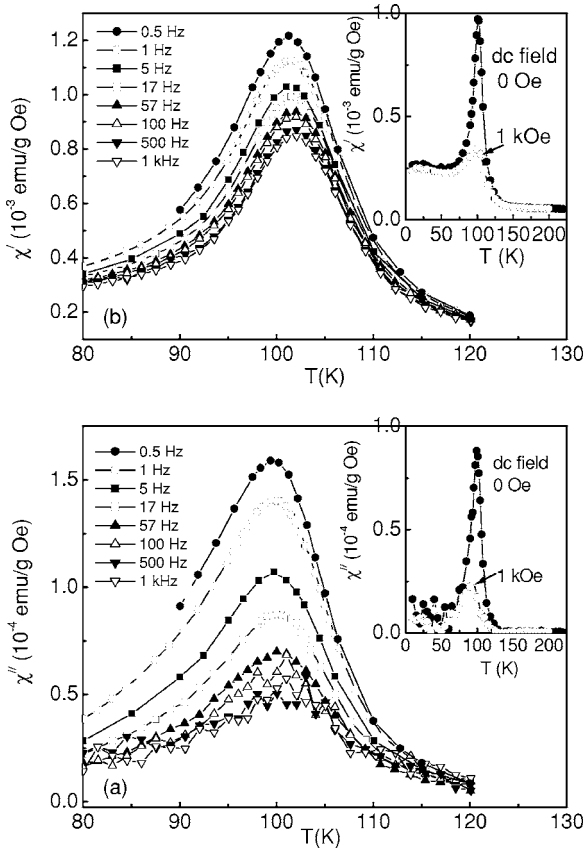

FIG. 2. Temperature dependence of the real part (a) and imaginary part (b) of ac susceptibility at $h_{rms}=1$ Oe for different frequencies. The insets compare the ac susceptibility data for 10 Hz in presence and absence of superimposed 1 kOe dc field with $h_{rms}=1$ Oe.

magnetic field [inset of Fig. 2(a) and Fig. 2(b)] superimposed with the ac field ($h_{rms}=1$ Oe, frequency=10 Hz) reduces the magnitude of peak value alone, without shifting the (χ' and χ'') peak position in the temperature scale. One more interesting feature is that magnitude of χ' shows usual decrease with increasing frequency, but the decrease of χ'' with increasing frequency is not consistent with conventional spin-glass system.[24] (In general magnitude of χ' decreases and χ'' increases with the increase of ac frequencies for glassy systems.) The unusual frequency response of χ'' is further examined from the measurement of $\chi(T,f)$ with frequencies (Fig. 3) in the temperature range 90 K–110 K. Both χ' (Fig. 3) and χ'' (not plotted in the figure) show a sharp increase at lower frequencies and their responses are almost frequency independent above 100 Hz. The observed frequency response of ac susceptibility rules out the possibility of spin-glass-like freezing below 100 K on the time scale of applied ac field frequencies. Inset of Fig. 3 indicates that low frequency regime (i.e., long time domain) of the Argand diagram (χ'' vs χ' plot as a function of frequencies at a constant temperature) is important for strong interacting spin dynamics of the present system.

The $M(H)$ measurement could be useful here to understand the magnetic order as well as the anisotropy effect on spin dynamics in the system. Figure 4(a) shows the $M(H)$

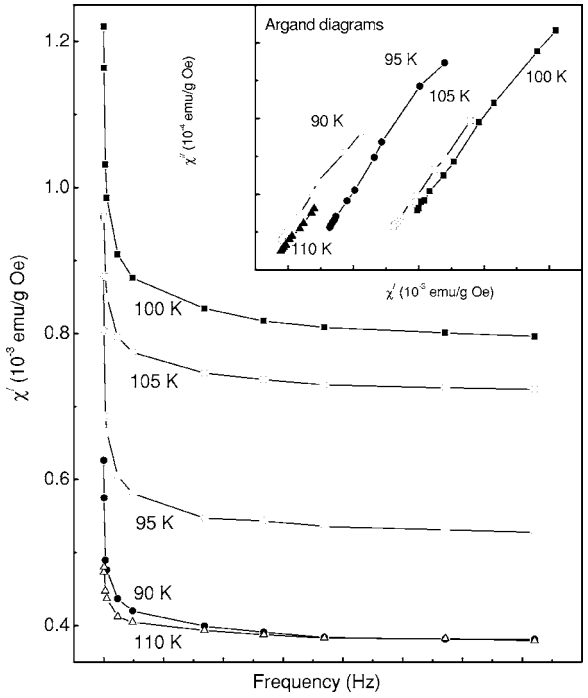

FIG. 3. ac susceptibility (real part) vs frequency at different temperatures. Inset shows Argand diagrams (χ'' vs χ' plot) for different temperatures.

data at diffierent temperatures and the features are similar to $MnCo_2O_4$.[16] The data show prominent field induced magnetic behavior (revealed by S shape) at lower temperatures, which becomes less prominent as the measurement temperature increases. Although a nonlinear increase of $M(H)$ is observed above 100 K, the analysis of Arrot plot (M^2 vs H/M at a constant temperature) [Fig. 4(b)] shows no spontaneous magnetization above 100 K, indicating paramagnetic state of the system. The data [Fig. 4(c)] also show no hysteresis loop at $T \geqslant 100$ K, whereas symmetric hysteresis loops are observed for temperatures below 100 K. Hysteresis loop at all temperatures are obtained for applied field $H=\pm 70$ kOe, but data are shown in Fig. 4(c) for field ±40 kOe. We have estimated the coercive field H_C, where magnetization changes sign, and isothermal irreversibility field H_{irr}, below which loop is opened in $M(H)$ data. The large value of coercive field (H_C) (~22 kOe at 2 K and ~10 kOe at 10 K) of the present system is also comparable to other anisotropic ferromagnet.[25] We have compared in Fig. 4(d) the temperature (T) dependence of H_C, H_{irr}, M_S from $M(H)$ data, and the field (H) dependence of T_p and T_{irr} from $M(T)$ data. The data shows that H_C, H_{irr}, and M_S increases with the decrease of temperature, whereas T_p and T_{irr} decreases with the increase of field. The comparative (H_C, H_{irr}, M_S, T_p, and T_{irr}) data show a good indication of Curie temperature T_C at about 100 K, where the system changes from ferrimagnetic state to paramagnetic state above 100 K. However, $T_{irr}(H)$ data, along with the nonlinear increase of $M(H)$ data, suggested a true paramagnetic state only above 150 K and in between 100 K and 150 K, a short range magnetic correlation exists in the paramagnetic state. The other notable feature of the comparative [$T_p(H)$ and $H_C(T)$] data is that as long as the

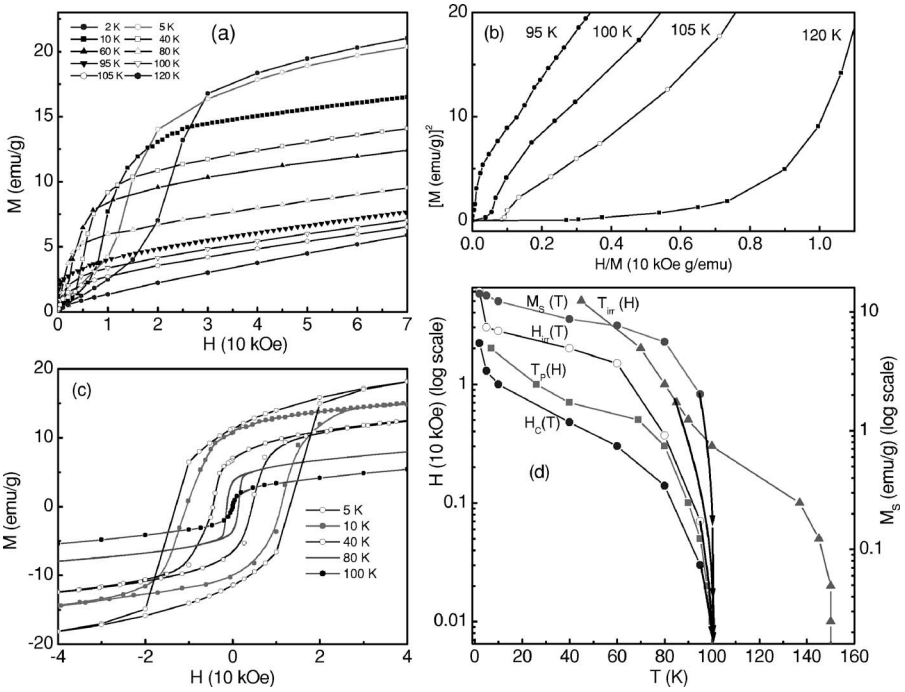

FIG. 4. (a) $M(H)$ data at different temperatures. (b) Arrot plot for selected temperatures. (c) $M(H)$ loop for selected temperatures. (d) Temperature dependence of H_C, H_{irr}, M_S and field dependence of T_p, T_{irr}.

measurement field is not large enough comparing the H_C values, a sharp MZFC peak may be observed and magnetization of the sample remains below of its saturation level at measurement temperatures below T_p. We can verify the above statement for $M(T)$ data at 2 K, where $H_C \sim 22$ kOe and $H_{\mathrm{irr}} \sim 60$ kOe. The $M(T)$ data (in Fig. 1) do not show any decrease for $H=50$ kOe ($H > H_C$), but sharp decrease is observed for $H=20$ kOe ($H < H_C \sim 22$ kOe). Such high field $M(T,H)$ behavior is consistent with the experimental results of other anisotropic ferrimagnets,[16,25] where it has been argued that shape of the MZFC maximum, in particular sharp decrease of MZFC is related to the domain wall pinning effect. The broadening of the peak about T_p and its shifting to lower temperatures with increasing field $H \geqslant 200$ Oe, similar to $MnCo_2O_4$,[16,17] is the indication of slow domain wall motion[26] in our system. Such domain wall motion is controlled by a field induced depinning transition at T_p where domain wall velocity acts as an order parameter.[27]

B. Magnetic order and electrical conductivity

We have measured dc conductivity and ac conductivity of the system in order to understand the effect of magnetic order on electrical conductivity. The results are discussed below.

1. dc conductivity

The dc resistivity in absence of magnetic field is shown in Fig. 5(a). The resistivity (ρ) continues to increase below 300 K as the temperature decreases down to 80 K, where a peak is observed in $\rho(T)$ data. This marks the transition from a semiconductor (above 100 K) to a metalliclike behavior below $T_{SM} \sim 80$ K. The result suggests that semiconductor-metal transition temperature ($T_{SM} \sim 100$ K) in $MnCo_2O_4$ (Ref. 10) is reduced to 80 K after 50% Ru substitution in Mn sites. We have also noted that Ru substituted sample shows further increase of resistivity below 40 K. We have analyzed the $\rho(T)$ data using a universal form,[28]

$$\rho(T) = \rho_0(T)\exp[(T_0/T)^s], \tag{1}$$

where the prefactor $\rho_0(T)=AT^m$ (m is another constant) and T_0 is a characteristic temperature. The exponent $s=1$ for nearest neighbor (thermal activated) hopping with activation energy $E_a=k_BT_0$ and obeys Arrhenius law, while $s=1/4$ and $1/2$ implies for variable range hopping (VRH) conductivity according to Mott[29] and Shklovskii and Efros (SE)[30] mechanisms, respectively. Fit of the $\ln\rho$ vs $1/T$ data [Fig. 5(b)] above 150 K to Arrhenius law gives activation energy $E_a \approx 0.10$ eV. The estimated activation energy is less in comparison with the commonly reported value >0.2 eV for insulating spinel oxides.[31] The resistivity of the present system at 300 K is only a few ohm cm (i.e., high conductivity) in comparison with resistivity $\sim 10^6$ ohm cm usually observed in spinels. The low value of the activation energy E_a, as well as higher conductivity in the semiconducting state, indicates that the present ferrimagnetic spinel belongs to the class of a good ferrimagnetic semiconductor.[11] From $\ln\rho$ vs $T^{-1/4}$ plot [Fig. 5(c)] we find that $s=1/4$ is a good exponent in the range 90 K to 240 K and the data above 240 K deviates from the fit. On the other hand, $\ln\rho$ vs $T^{-1/2}$ plot [Fig. 5(d)] shows that $s=1/2$ is the good exponent in the range 110 K to 300 K. Our analysis shows that variable range hopping conductivity (via small polaron formation) beyond the nearest neighbor sites is energetically favorable above 100 K. The decrease of resistivity [Fig. 5(a)] in the presence of 8 kOe magnetic field below 100 K indicates that the small polarons have spin character and magnetic order affecting the polaron conductivity. The system also shows [in the inset of Fig. 5(a)] large magnetoresistance MR(%){=[$\rho(0) - \rho(8\ \mathrm{kOe})] \times 100/\rho(0)$}, with a maximum $\sim$48% at 80 K

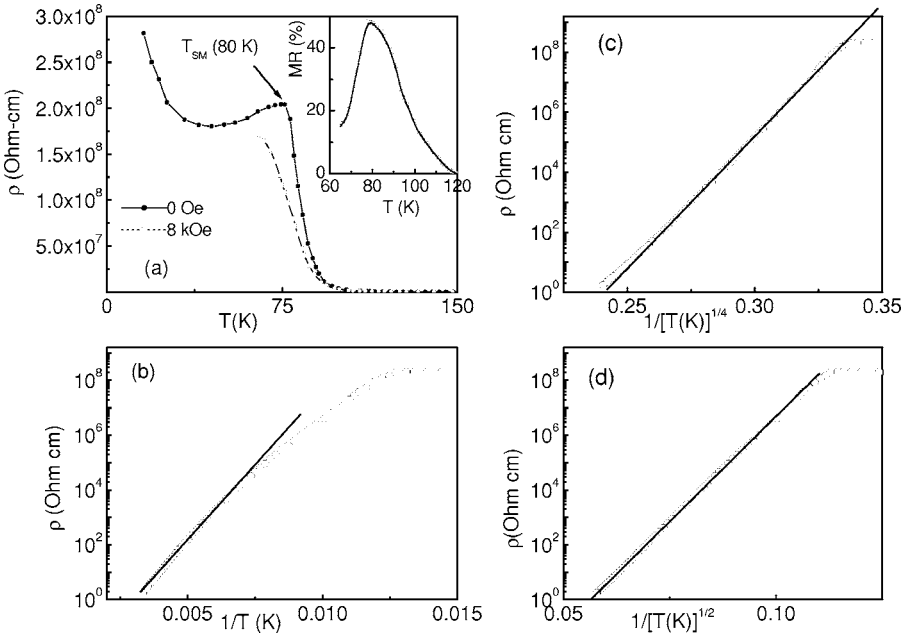

FIG. 5. (a) Temperature (T) dependence of resistivity (ρ) data with and without magnetic field. T_{SM} (80 K) is the semiconductor to metallic transition temperature. Inset of (a) shows the MR values calculated from $\rho(0)$ and $\rho(8\ \text{kOe})$ data. Analysis of $\rho(T)$ data according to $\rho = \rho_0 \exp(E_a/k_B T)$ (Arrhenius law) [in Fig. 5(b)], ρ vs $1/T^{1/4}$ [in Fig. 5(c)], ρ vs $1/T^{1/2}$ [in Fig. 5(d)]. Lines are drawn for guide to eye.

and becomes less than 1% above 120 K. This suggests the persistent of the CMR effect even after 50% Ru substitution in Mn sites of $MnCo_2O_4$.[16]

2. ac conductivity

We have investigated the real part of ac conductivity (σ_p) in the temperature range 16 K to 300 K, covering paramagnetic state to ferrimagnetic state. σ_p can be written as $\sigma_p = \sigma_0 + \sigma(f)$, where σ_0 is the dc conductivity (at the $f=0$ Hz frequency limit of ac conductivity) and $\sigma(f)$ is the frequency activated component of ac conductivity. The ac conductivity (σ_p) vs frequency (f) data (log-log scale) are shown in Fig. 6. There is an overall increase of ac conductivity with the increase of frequency, as well as with the increase of temperature. We noted that ac conductivity of the system has shown a frequency dependence over the measurement range 17 Hz to 1 MHz. The ac conductivity below 100 K are almost independent of temperatures, except a small variation in σ_0. The data follow a power law $\sigma_p \sim f^n$ behavior with $n \approx 0.96$ for the whole frequency range. On further increase of temperature a systematic deviation is observed, where a low frequency regime is clearly distinguished from the high frequency regime satisfied by n always below 0.96. Note that ac conductivity of the system is not frequency independent, also seen in some spinel,[22] in the low frequency regime. The response of ac conductivity in low frequency regime is small for temperatures above 150 K (e.g., $n \approx 0.03$ at 176 K and 0.016 at 230 K for $f < 500$ Hz). The ac conductivity of the present system becomes negligibly frequency dependent (e.g., $n \approx 0.0002$ at 300 K) in the low frequency regime only for $T \gg T_C$. We have seen that fit values of n (from higher frequency regime) decreases with the increase of temperature. For example, $n \approx 0.91$ at 176 K, 0.62 at 230 K, and 0.33 at 300 K. Similar decrease of n is consistent with the literature.[22,32] We have shown normalized σ_p/σ_0 vs (f/f_C)

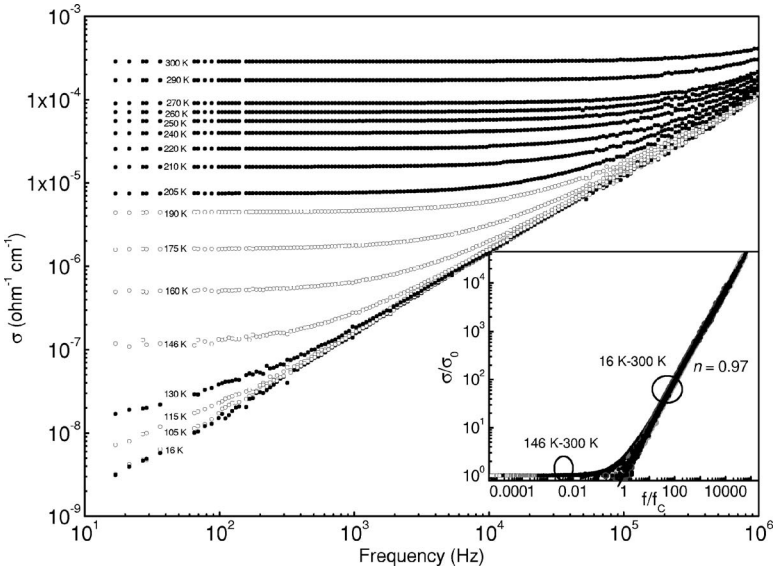

FIG. 6. Frequency dependence of ac conductivity data at different temperatures. Inset shows the normalized ac conductivity (σ/σ_0) vs normalized frequency (f/f_C) for the temperature range 16 K–300 K. All the data above f_C are scaled with an exponent 0.97. Also note that the data for all temperatures above 146 K are scaled to a single master curve, whereas the data for temperatures below 146 K are deviated in the low frequency regime from the master curve.

data in the log-log scale (inset of Fig. 6), where σ_0 is the dc conductivity estimated from the extrapolation of ac conductivity data down to dc ($f=0$ Hz) limit. f_C is the suitable frequency needed to scale the ac conductivity data at different temperatures and may be nearly equal to the crossover frequency from low frequency dependent regime to high frequency activated regime.[32] The ac conductivity at $f \geqslant f_c$ are scaled to

$$\sigma_p/\sigma_0 \sim (f/f_C)^n \tag{2}$$

with scaling exponent $n=0.97$ for all the temperatures. We have seen (inset of Fig. 6) that below scaling frequency (f_C) nonlinearity starts in the scaling plot and ac conductivity data for $T \geqslant 146$ K falls in a single curve, whereas the data for $T<130$ K gradually deviate from the non-linear master curve towards the straight line with $n=0.97$ for $T=16$ K. Both σ_0 and f_C depends on temperature. Interestingly both are correlated, irrespective of temperatures, by a simple power law

$$\sigma_0 \sim f_C^{1.38}. \tag{3}$$

Here, σ_0 and f_C are not monotonically decreasing with temperature. They show a minimum at about 100 K, where a peak in the ac susceptibility data has been observed.

IV. DISCUSSION

The magnetic measurement, as well as the ac conductivity scaling, shows long range ferrimagnetic order of $Mn_{0.5}Ru_{0.5}Co_2O_4$ spinel oxide below $T_C \sim 100$ K. The observation of large magnetic irreversibility between zero field cooled and field cooled magnetization of the sample is due to the presence of large magnetocrystalline anisotropy, originated from Co^{2+} ions located in A sublattice of $Mn_{0.5}Ru_{0.5}Co_2O_4$.[19] The magnetic irreversibility is observed above T_C (i.e., $T_C \leqslant T_{irr}$) for low field measurements. The difference $\Delta T(=T_{irr}-T_p)$ is nearly 50 K [taking $M(T)$ data at 10 Oe] for the present sample, which is large in comparison with $\Delta T \approx 11$ K (before Ru substitution) in $MnCo_2O_4$.[16] This suggests that substitution of Ru for Mn in $MnCo_2O_4$ introduces some magnetic disorder. Recently, neutron diffraction measurements[21] also suggested the existence of short range magnetic order below 150 K. Experimental results show that the magnetic disorder in the present sample is not well enough for the exhibition of spin-glass-like behavior, as seen in $RuCo_2O_4$.[19] The origin of the magnetic disorder and its effects in details are discussed below.

Neutron experiment suggested the existence of three B sublattice cations (Co^{3+}, Mn^{3+}, and Ru^{3+}) in $Mn_{0.5}Ru_{0.5}Co_2O_4$. Among the possible B sublattice cations, Ru^{3+} is low spin moment ($S=1/2$) and Co^{3+} is nonmagnetic ($S=0$). The substitution of Ru (low spin moment) in Mn sites replaces the equivalent amount of strong intersublattice $Co^{2+}(A)$--O^2-$Mn^{3+}(B)$ bonds by $Co^{3+}(A)$-O^{2-}-$Ru^{3+}(B)$ bonds, which reduces the ferrimagnetic order in the system. The possibility of valence fluctuations among B sublattice cations can alter the magnetic interactions[10,13–15] via the formation of the following superexchange bonds: Co^{3+}-O^{2-}-Co^{3+}, Co^{3+}-O^{2-}-Mn^{3+}, Co^{2+}-O^{2-}-Mn^{4+}, Co^{3+}-O^{2-}-Ru^{3+}, Mn^{3+}-O^{2-}-Mn^{3+}, Mn^{3+}-O^{2-}-Ru^{3+}. The nonuniform distribution of magnetic and nonmagnetic superexchange bonds creates B sublattice disorder, which favour the formation of short range interacting clusters even in the paramagnetic state.[33] Such clusters, associated with electrical charge carriers, are known as polarons. Conductivity in spinel compound, having no direct covalent bond between cations, are largely controlled by hopping mechanism of charge carriers.[10,16,19] The probable charge transfer may occur between Co (Co^{3+}/Co^{2+}) ions and Mn (Mn^3/Mn^{4+}) ions.[10,13–16]

The fluctuation effect from B sublattice magnetic exchange interactions, in addition to the fluctuation in Coulomb potential, has shown a large impact on the variable range hopping (VRH) conductivity above T_C. The observation of magnetoresistance (MR) below 150 K may be small, but finite, and confirmed the existence of short range interacting clusters in the paramagnetic state. As the temperature decreases below 150 K, the system may have many short range interacting clusters. The size of the clusters are increased due to the increasing interactions among the clusters until the interactions are saturated below 100 K and the clusters begin to melt in the long range ferrimagnetic matrix. Such picture of magnetic clusters can be compared with the breaking down of polarons into naked charge carriers in the ferrimagnetic state, as suggested for other CMR spinel.[34] The polarons may exist above 150 K, but magnetic polarons are associated with magnetic short range interactions below 150 K and we equivalent them to the magnetic clusters. The present sample shows a large magnetoresistance (CMR) below 100 K with a semiconductor to metallic transition temperature at $T_{SM} \sim 80$ K. It is the fact that there is a difference of 20 K between ac susceptibility (T) peak and resistivity (T) (in absence of magnetic field) peak. However, such difference is also observed in other CMR spinel compounds, like $FeCr_2S_4$ (Refs. 6 and 34) and $MnCo_2O_4$.[10] On the other hand, the magnetic behavior in the present sample below T_C is largely controlled by the domain wall pinning effect. We have seen that depinning of the domain wall is activated either at low frequency regime of ac susceptibility measurements or at higher magnetic field of dc magnetization measurements.

We can understand the magnetic order in the context of ac conductivity data. The power law behavior of the frequency activated component of ac conductivity with exponent less than 1 suggests the hopping conduction of localized (bound) charge carriers. Such hopping conduction is affected by the interaction between cations and their surroundings, which may not be restricted to the nearesr neighbors only. For example, response of a magnetic system to electric field depends not only upon the nonmagnetic interactions, such as Coulomb potentials, etc., but also on the magnetic order of the cations (spin moments). The experimental data indicated such a distribution of interactions, arisen due to nonuniform distribution of B site cations in our system, above the ferrimagnetic ordering temperature. The existence of such a broad range of interactions has been favored for the variable range hopping conductivity above T_C.

Finally, we show a comparative plot (Fig. 7) between the temperature dependence of dc conductivity ($1/\rho$: from resis-

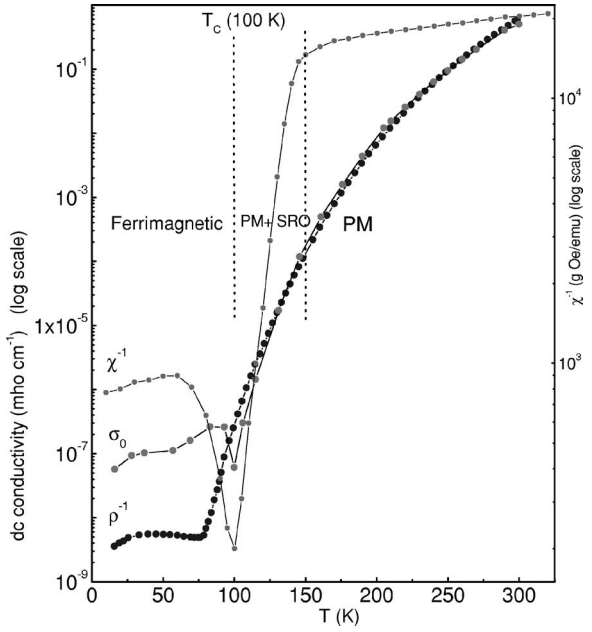

FIG. 7. Comparative plot for the temperature dependence of the inverse of dc conductivity (ρ^{-1}), ac conductivity at the zero frequency limit (σ_0) needed for the ac conductivity scaling and inverse of dc susceptibility (χ^{-1}) at 10 Oe (right y axis). The dotted lines guide the separation between ferrimagnetic state, paramagnetic state (PM) mixed with short range magnetic order (SRO), and paramagnetic state (PM).

tivity measurement), ac conductivity at the zero frequency limit (σ_0), and inverse of dc suseptibility (χ_{dc}^{-1}: from dc magnetization measurement at 10 Oe) data. We find that the values of σ_0 needed for ac conductivity scaling are nearly matching with dc conductivity from direct resistivity measurement in absence of magnetic field, except ceratin deviation below 100 K. For example, the minimum of dc conductivity data in absence of magnetic field occurs at $T_{SM} \sim 80$ K, which is low in comparison with the location of the minimum of σ_0 near to 100 K. In spite of the existence of small quantitative deviation, the nature (or shape) of $1/\rho$ (T) and σ_0 (T) are qualitatively identical at low temperatures. More interestingly the temperature of the σ_0 (T) minimum matches with the minimum of χ_{dc}^{-1} (T) data near to the paramagnetic to ferrimagnetic ordering temperature (T_C) ~ 100 K for the system. Similarly, the deviation of dc conductivity from Arrhenius law (due to the increasing contribution of variable range hopping conductivity of polarons) is comparable to the deviation of χ (T) data from Curie-Weiss law (due to the increasing short range magnetic interactions to magnetic ordering) below 150 K. The comparative plot shows that scaling of the ac conductivity is guided by the different magnetic states (paramagnetic above 150 K, paramagnetic mixed with short range magnetic interactions at $150\ \mathrm{K} > T > 100$ K, and long range ferrimagnetic state below 100 K) in $Mn_{0.5}Ru_{0.5}Co_2O_4$ spinel oxide.

V. CONCLUSION

The substitution of 50% Mn by Ru in $MnCo_2O_4$ has resulted in the decrease of ferrimagnetic ordering temperature from 180 K in $MnCo_2O_4$ to 100 K in $Mn_{0.5}Ru_{0.5}Co_2O_4$. The magnetic disorder in B sublattice is not sufficient to show a spin-glass behavior in $Mn_{0.5}Ru_{0.5}Co_2O_4$. Although a difference between ZFC and FC magnetization curves appeared below 150 K, the experimental data indicated a true long range ferrimagnetic state below the Curie temperature (T_C) at 100 K. The magnetic behavior below T_C is controlled by the effect of strong anisotropy and domain wall pinning. The paramagnetic state above 100 K can be divided into two regions, i.e., a true paramagnetic state above 150 K and a paramagnetic state mixed with short range interactions below 150 K. The observation of significant magnetoresistance (with maximum $\sim$48% at 80 K) below the ferrimagnetic ordering temperature suggests a close coupling between magnetic order and electrical conductivity in the system. The onset of magnetic correlation among the spins in the paramagnetic state, as well as the saturation of magnetic order below T_C is well understood by a simple ac conductivity scaling.

ACKNOWLEDGMENTS

The authors thank R. Nagarajan and Chandan Mazumdar for useful discussion.

*Corresponding author; Present address: Department of Physics, Pondicherry University, R.V. Nagar, Kalapet, Pondicherry-605014, India. Electronic address: rabindranath.bhowmik@saha.ac.in

†Electronic address: r.ranganathan@saha.ac.in

[1] R. N. Bhowmik, R. Nagarajan, and R. Ranganathan, Phys. Rev. B **69**, 054430 (2004).

[2] R. N. Bhowmik, R. Ranganathan, and R. Nagarajan, Phys. Rev. B **73**, 144413 (2006).

[3] A. S. Risbud, R. Seshadri, J. Ensling, and C. Felser, J. Phys.: Condens. Matter **17**, 1003 (2005).

[4] V. A. M. Brabers, in *Handbook of Magnetic Materials*, edited by K. H. J. Buschow (North-Holland, Amsterdam, 1995), Vol. 8, p. 189.

[5] R. C. O'Handley, *Modern Magnetic Materials: Principles and Applications* (Wiley, New York, 2000).

[6] A. P. Ramirez, R. J. Cava, and J. Krajewskyki, Nature (London) **386**, 156 (1997).

[7] E. Schmidbauer, Solid State Commun. **12**, 507 (1973).

[8] K. P. Belov, Phys. Usp. **37**, 563 (1994).

[9] J.-M. Li, A. C. H. Huan, L. Wang, Y.-W. Du, and D. Feng, Phys. Rev. B **61**, 6876 (2000).

[10] J. Philip and T. R. N. Kutty, Mater. Lett. **39**, 311 (1999).

[11] M. Ziese, Rep. Prog. Phys. **65**, 143 (2003).

[12] J. A. Alonso, J. L. Martinez, M. J. Martinez-Lope, M. T. Casais, and M. T. Fernandez-Diaz, Phys. Rev. Lett. **82**, 189 (1999).

[13] J. M. D. Coey, M. Viret, and S. Von Molnar, Adv. Phys. **48**, 167 (1999).
[14] G. Blasse, Philips Res. Rep. **18**, 38 (1963).
[15] E. E. Vainshtein, R. M. Ovrutskaya, and B. I. Kotlyar, Sov. Phys. Solid State **7**, 1707 (1966).
[16] P. A. Joy and S. K. Date, J. Magn. Magn. Mater. **210**, 31 (2000); **218**, 229 (2000).
[17] F. M. M. Borges, D. M. A. Melo, M. S. A. Camara, A. E. Martinelli, J. M. Soares, J. H. de Araujo, and F. A. O. Cabral, J. Magn. Magn. Mater. **302**, 273 (2006).
[18] G. N. Banerjee, R. N. Bhowmik, and R. Ranganathan, J. Phys.: Condens. Matter **13**, 9481 (2001).
[19] D. Mandrus, V. Keppens, and B. C. Chakoumakos, Mater. Res. Bull. **34**, 1013 (1999).
[20] V. Antropov, Phys. Rev. B **72**, 140406(R) (2005).
[21] G. E. Granroth, D. Mandrus, V. Keppens, and S. E. Nagler, J. Magn. Magn. Mater. **272-276**, 1306 (2004).
[22] P. Lunkenheimer, R. Fichtl, J. Hemberger, V. Tsurkan, and A. Loidl, Phys. Rev. B **72**, 060103(R) (2005).
[23] J. S. Smart, Am. J. Phys. **23**, 356 (1955).
[24] D. Hüser, L. E. Wenger, A. J. van Duyneveldt, and J. A. Mydosh, Phys. Rev. B **27**, 3100 (1983).
[25] C. Mazumdar, R. Nagarajan, L. C. Gupta, B. D. Padalia, and R. Vijayaraghavan, Appl. Phys. Lett. **77**, 895 (2000).
[26] O. Petracic, A. Glatz, and W. Kleemann, Phys. Rev. B **70**, 214432 (2004).
[27] L. Roters, A. Hucht, S. Lübeck, U. Nowak, and K. D. Usadel, Phys. Rev. E **60**, 5202 (1999).
[28] R. Laiho, K. G. Lisunov, E. Lähderanta, V. S. Stamov, V. S. Zakhvalinskii, Ph Colomban, P. A. Petrenko, and Yu P. Stepanov, J. Phys.: Condens. Matter **17**, 105 (2005); R. Laiho, K. G. Lisunov, E. Lähderanta, P. A. Petrenko, J. Salminen, M. A. Shakhov, M. O. Safontechik, V. S. Stamov, M. V. Shubnikov, and V. S. Zakhvalinskii, *ibid.* **14**, 8043 (2002).
[29] N. F. Mott, *Metal-Insulator Transitions* (Taylor and Francis, London, 1990).
[30] B. I. Shklovskii and A. L. Efros, *Electron Properties of Doped Semiconductors* (Springer, Berlin, 1984).
[31] S. J. Yoon, S. H. Lee, K. H. Kim, and K. S. Ahm, Mater. Chem. Phys. **73**, 330 (2002).
[32] J. C. Dyre and T. B. Schroder, Rev. Mod. Phys. **72**, 873 (2000).
[33] H. D. Zhou and J. B. Goodenough, J. Phys.: Condens. Matter **17**, 7395 (2005).
[34] Z. Yang, S. Tan, and Y. Zhang, Phys. Rev. B **64**, 024401 (2001).